CHAPTER 238

NUMERICAL MODEL OF THE NONLINEAR INTERACTION OF WAVES AND FLOATING BODIES

Michael Brorsen [1] Henrik I. Bundgaard [2]

Abstract

A numerical model for the computation of the nonlinear interaction of water waves and floating large-volume bodies is described. The model works in the time domain and is based on the boundary element method (BEM) with internal generation of the incident waves and absorption of all outgoing waves (internally generated as well as reflected). This procedure makes it possible to simulate long time series of nonlinear wave forces even in case of irregular waves. Drift forces are extracted from the time series by filtering. Steady and slowly varying drift forces are computed in 2D and first order wave forces are computed in 3D.

Introduction

The need for an accurate description of the interaction of nonlinear water waves with floating large-volume bodies has been increasing during the last decade. The forces acting on a floating body are generally divided into three components:

- forces at wave frequencies.
- low-frequency forces caused by e.g. wave groups.
- steady components of the forces.

In most (if not all) commercial models today the wave-body interaction is based on linear theory in the frequency domain. This approach leads normally to accurate estimates of the forces at wave frequencies. The estimates of the two nonlinear components of the forces are, however, usually less accurate and only available up to second order.

Especially the low-frequency force is difficult to estimate from the linear theory. See e.g. Standing (1981). These forces are denoted slowly varying drift forces in this paper.

[1]University of Aalborg, Sohngaardsholmsvej 57, DK-9000 Aalborg, Denmark
[2]Danish Hydraulic Institute, Agern Alle 5, DK-2970 Hørsholm, Denmark

All nonlinear effects which can be described by potential theory can be taken into account by the approach presented here. This is achieved by the fulfilment of the nonlinear boundary conditions at the free surface and integration of the nonlinear pressure forces up to the free surface.

Isaacson (1982) applied a very similar approach, but it was not possible to simulate long time series. Scattered waves were reflected back into the domain from that part of the boundary, where the incident waves were generated. In order to avoid this problem either a very long computational domain or a spatially periodic boundary condition has been applied.

The application of a long domain is very costly as it generates a large system of equations and the spatially periodic boundary condition is only an approximation in most cases with a body of arbitrary shape.

If the incident waves are generated inside the computational domain all waves reaching the domain boundaries are per definition outgoing waves. At the open boundaries these waves can be absorbed and the wave field inside the domain is not corrupted by scattered waves reflected at the boundaries. This approach was introduced for the BEM method by Brorsen and Larsen (1987) and it makes it possible to simulate time series as long as necessary to determine the slowly varying drift forces as well as the steady drift force.

It should be stressed that this approach is applicable in both 2D and 3D models.

The 2D version of the model is used to calculate the drift forces on a rectangular body in case of regular waves and beating waves.

The 1. order wave forces on a barge are calculated by the 3D version of the model.

Theoretical formulation

Fluid flow

Irrotational flow of an incompressible and inviscid fluid is considered. Therefore a velocity potential φ exists, giving the fluid velocity $\vec{v}$ as

$$\vec{v} = \nabla\varphi \tag{1}$$

The incident waves are generated by a vertical source distribution situated between the floating body and the open boundary of the domain.

The time varying volume flux density of the source distribution is denoted q^*, and the velocity potential φ must satisfy the Poisson equation

$$\nabla^2\varphi = q^*(\vec{\zeta}, t) \tag{2}$$

where $\vec{\zeta}$ is the position vector of the source and t is the time.

Brorsen and Larsen (1987) has described how q^* should be varied in space and time in order to generate a specified incident wave field.

On the free surface the nonlinear kinematic and dynamic boundary conditions are fulfilled, i. e.

$$\frac{\partial \varphi}{\partial n} \cdot \frac{1}{cos\beta} = \frac{\partial \eta}{\partial t} \quad \text{at} \quad z = \eta \tag{3}$$

$$\frac{\partial \varphi}{\partial t} + gz + \frac{1}{2}(\nabla \varphi)^2 = 0 \quad \text{at} \quad z = \eta \tag{4}$$

where β is the angle between the outward normal to the free surface and the vertical direction, g is the gravitational acceleration, z is the level of the point.

On the sea bed the no flow condition is used,

$$v_n = \frac{\partial \varphi}{\partial n} = 0 \quad \text{at} \quad z = -h \tag{5}$$

On the surface of the floating body it is assumed that the body and the fluid have the same velocity component in the direction of the normal to the body, i.e.

$$\frac{\partial \varphi}{\partial n} = \vec{v}_b \cdot \vec{n} \quad \text{on} \quad S_b \tag{6}$$

where $\vec{v}_b$ is the velocity of a point on the surface of the body and S_b denotes the instantaneous wetted surface of the body.

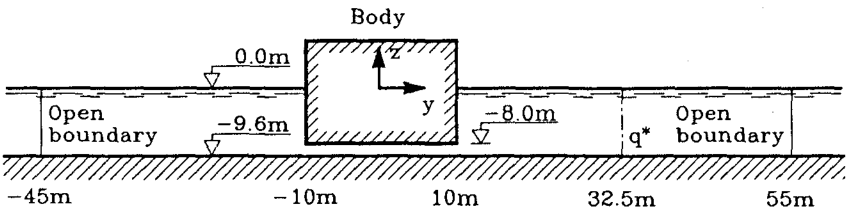

Figure 1. Sketch of 2D wave channel and floating body. Still water.

The domain is enclosed by vertical open boundaries, see Fig 1., where all outgoing waves are absorbed. The absorption is modelled with the radiation condition:

$$\frac{\partial \varphi}{\partial t} = -c\frac{\partial \varphi}{\partial n} \tag{7}$$

where c is the phase velocity. The radiation condition is nonreflecting in case of waves of constant form propagating out of the domain. This boundary condition is, however, found to be adequate also in case of beating waves provided that the wave periods do not deviate substantially from each other, i.e. the rate of change in form is rather small.

The forces from the fluid on the body is found by integration,

$$\vec{F}_p = \int_{S_b} p\,\vec{n}\,dS \tag{8}$$

where S_b denotes the instantaneous wetted surface of the body and p the pressure. The pressure is obtained from the nonlinear Bernoulli's equation:

$$\frac{\partial\varphi}{\partial t} + gz + \frac{1}{2}(\nabla\varphi)^2 + \frac{p}{\rho} = 0 \tag{9}$$

where ρ is the density of the fluid.

We need to calculate the pressure at points moving with the velocity $\vec{v}_{point}$. In that case, see e.g. Brorsen (1989), equation (9) reads:

$$p = -\rho gz + \rho\frac{d\varphi}{dt} + \rho\vec{v}_{point}\cdot\nabla\varphi - \frac{1}{2}\rho(\nabla\varphi)^2 \tag{10}$$

The boundary value problem is transformed into an integral equation by the application of Green's 2. identity.

Thus the potential at point P positioned at $\vec{x}$ is given by

$$\alpha\cdot\varphi(\vec{x}) = \int_S\left(\varphi(\vec{\xi})\frac{\partial G(\vec{x},\vec{\xi})}{\partial n} - G(\vec{x},\vec{\xi})\frac{\partial\varphi(\vec{\xi})}{\partial n}\right)dS + \int_A q^*(\vec{\zeta},t)G(\vec{x},\vec{\xi})dA \tag{11}$$

where S is the boundary of the domain A, $\vec{\xi}$ denotes the position vector of a point on the boundary, $G(\vec{x},\vec{\xi})$ is a Green function and α is a constant.

In case of constant water depth and $\vec{x}$ is situated on the boundary of the domain, we use the following Green function:

$$\text{2D model} \;:\; \alpha = \pi \;\text{ and }\; G(\vec{x},\vec{\xi}) = ln\left|\vec{\xi}-\vec{x}\right| + ln\left|\vec{\xi}-\vec{x}_r\right|$$

$$\text{3D model} \;:\; \alpha = -2\pi \;\text{ and }\; G(\vec{x},\vec{\xi}) = \frac{1}{\left|\vec{\xi}-\vec{x}\right|} + \frac{1}{\left|\vec{\xi}-\vec{x}_r\right|}$$

where $\vec{x}_r$ is the position vector of the point which is the reflection of point P into the sea bed.

Motions of the body

In 3D the body has the 6 degrees of freedom shown in Fig. 2. Only 3 degrees of freedom are present in 2D, namely sway, heave, and roll.

The motions of the body are found from the equations of motion expressed in a coordinate system with origo at the center of gravity (CG) and fixed to the body, i.e.:

$$\sum\vec{F}_{external} = m(\dot{\vec{v}}_G + \vec{\omega}\times\vec{v}_G) \tag{12}$$

$$\sum\vec{M}_{external} = \bar{\bar{I}}\,\frac{d\vec{\omega}}{dt} + \vec{\omega}\times(\bar{\bar{I}}\,\vec{\omega}) \tag{13}$$

where $\vec{v}_G$ is the velocity of CG and $\vec{\omega}$ is the angular velocity of the body. $\overline{\overline{I}}$ is the matrix of moment of inertia and m the mass of the body. $\vec{F}_{external}$ and $\vec{M}_{external}$ denote external force and moment with respect to CG, respectively.

The external forces are pressure forces from the fluid, see equation (8), and e.g. forces from moorings, fenders and wind.

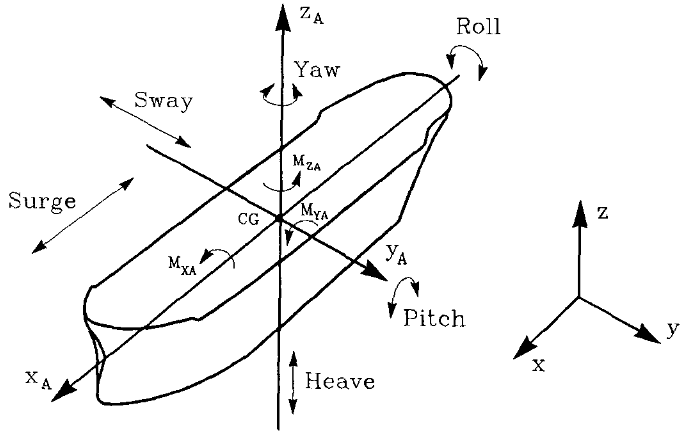

Figure 2. Definition sketch of surge, heave, roll, sway, pitch and yaw.

Numerical formulation

A time-stepping technique is used, where the flow problem is solved at each time level. Time-dependent terms are discretized as finite differences, and time step k is indicated with k as a superscript, i.e. φ^k denotes the velocity potential at the time $t = k\Delta t$, where Δt is the time step.

The boundary is discretized into N linear (in 2D) or plane (in 3D) elements and the variables φ, $\partial\varphi/\partial n$, p and η are calculated at points situated at the centroid (the node) of each element. It is, furthermore, assumed that the variables are constant over each element.

The pressure force on the body is calculated by the discretized version of equation (8), i.e.

$$\vec{F}_p = \sum_{j=1}^{N} p_j \vec{n}_j dA \tag{14}$$

where index j refers to a element on the body, p is the pressure at node j and $\vec{n}$ is the unit, outward normal to the body.

Note that equation (14) is exact if the pressure distribution over each element is linear.

It is now assumed that the flow, the velocity of the body and the position of the boundary are known at time step k. The unknown shape of the boundary at time step $k+1$ is estimated by a linear extrapolation, see Isaacson (1982). The first estimate of the flow at time step $k+1$ is found by application of equation (11) at each node. This gives N equations, which can be solved together with the discretized boundary conditions, see Brorsen and Larsen (1987). After the solution φ^{k+1} and $(\partial\varphi/\partial n)^{k+1}$ are known at all nodes. The pressure $p^{k+\frac{1}{2}}$ and the elevation η^{k+1} are known at the nodes on the body and the free surface, respectively.

When the values of $p^{k+\frac{1}{2}}$ are known, updated values of forces and moments from the fluid are calculated. This leads to the calculation of improved estimates of the position and velocity of the body by use of the discretized versions of equation (12) and (13).

Hereafter the free surface is updated according to the η^{k+1}-values, and the N equations are set up and solved once more. In this study only insignificant changes were observed if the procedure was repeated a 3. time.

In all simulations the fluid is at rest at time $t=0$.

Numerical example, 2D

The objective of this section is to show that it is possible to calculate the nonlinear wave forces on both fixed and floating bodies so accurately that the drift forces can be obtained by filtering of the raw force time series.

Rectangular body exposed to nonlinear regular waves

In this example a rectangular body with beam $b = 20\ m$ and draft $d = 8.0\ m$ is exposed to regular waves generated at $y = 32.5\ m$.

The drift forces on both a fixed body and a freely floating body are calculated.

The incident wave height H is varied between $0.2\ m$ and $0.9\ m$ and the applied wave period is constant $T = 8.0\ sec$ corresponding to a 1. order wave length $L = 69.8\ m$.

The water depth is $9.6\ m$ and the two open boundaries are radiation boundaries. See Fig. 1. The boundary is discretized into 41 elements, where the element length near the open boundaries is $5.0\ m$ decreasing to $2.0\ m$ on the body. The time step is $\Delta t = 0.5\ sec$ corresponding to only 16 steps per wave period.

The steady drift force on the body is calculated by a low pass filtering of the total lateral force found by equation (14). The numerical results are in Fig. 3 compared with the theoretical second order drift force derived by Longuet-Higgins (1977):

$$F_{drift} = \frac{1}{16}\rho g\left(1+\frac{2kh}{sinh2kh}\right)\left(H_i^2+H_r^2-H_t^2\right) \tag{15}$$

where $k = 2\pi/L$ and H_i, H_r, H_t are the incident, reflected, and transmitted wave heights, respectively.

H_r and H_t are estimated by Fourier analysis, and it is found that the numerical damping is insignificant, i.e. $H_i^2 \approx H_r^2 + H_t^2$.

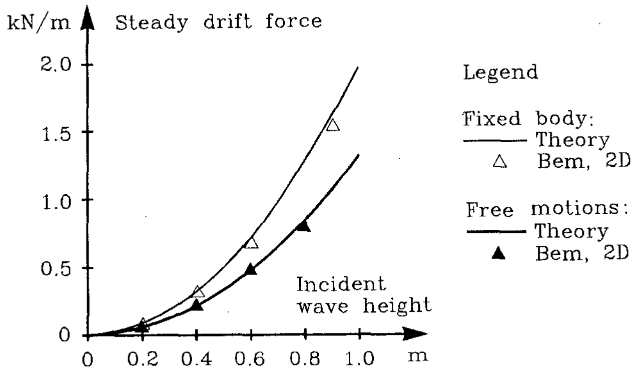

Figure 3. Comparison of calculated and theoretical steady drift force, 2D model.

From Fig. 3 is seen that the agreement between the numerical results and the theoretical solutions are excellent even though a steady drift force is only a few percent of the amplitude of the total lateral force (0.6% if $H_i = 0.20\ m$ in case of fixed body). Note that the floating body is more transparent to the waves than the fixed body.

Rectangular body exposed to a pair of nonlinear, beating waves

The mean drift force and the slowly varying drift force on a fixed body are calculated.

The domain and the body are the same as described in the preceding example. The two beating waves have each a wave height of 0.4 *m* and the periods are 8 and 10 *sec*, respectively. This gives a wave group period of 80 *sec* and the length between the nodes of the group is 302 *m*. The corresponding slowly varying drift force has a period of 40 *sec*.

In case of beating waves one must be careful to generate the correct bounded long wave in order to avoid spurious free long waves, see Stig Sand (1982). In this study this is done by including the velocities corresponding to the bounded long wave when the source distribution is calculated.

Initially it was checked that the correct bounded long wave (amplitude and phase) was created and that only insignificant reflection took place at the radiation boundary. This was done by calculation of the beating waves in a domain without the body. The bounded wave amplitude and phase were found by filtering of the elevation time series at several stations. Excellent agreement was found with the theoretical results, probably because the phase velocities of the short and long waves do not deviate to much in case of shallow water.

Note, however, that in a deep water situation, the larger deviations in phase velocities are expected to create a significant reflection on the radiation boundary. This will result in both wrong amplitude and phase of the long wave.

The slowly varying drift force on the body and the corresponding surface elevation 1.5 m upstream of the body are shown in Fig. 4. This drift force is found by application of a filter with a cut-off frequency of 0.04 Hz.

The mean value of the drift force is calculated to -0.59 kN/m. Note that the mean value of the drift force only deviates 2% from the theoretical value, -0.60 kN/m, which is the sum of the steady drift forces corresponding to the individual regular waves.

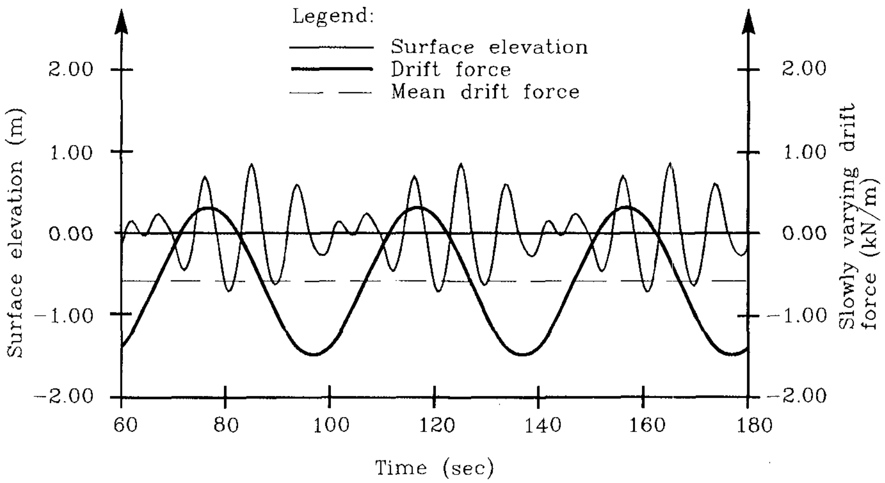

Figure 4. Slowly varying drift force on a fixed body. 2D model.

From Fig.4 is seen that the maximum drift force (negative) appears later than the maximum elevations in the wave group.

According to Newman's approximation the maximum drift force (negative) should appear at the same time as the max. elevations in the wave group. However, when the effect of the surface gradient of the bounded long wave is taken into account, it must be expected that the maximum drift force appears later than the maximum surface elevations and increase in magnitude.

The amplitude of the slowly varying drift force is seen to be approx. 30% bigger than the corresponding value according to Newman's approximation, which in this case is equal to the mean drift force.

A full verification of the computed results, e.g. by comparing the result with results from a theoretical 2. order model, see Faltinsen (1979), has not been made so far.

Linear 3D-Model (BEMSHIP)

At the Danish Hydraulic Institute a 3D model has been developed. This model calculates the motions in six degrees of freedom of a floating body. So far this model is based on the linearized equations, but non-linear mooring forces and fender forces can easily be included.

3D ship movements calculated by BEMSHIP are in the following compared to some test values, see Östergaard (1987).

The 'ship' selected is a rectangular barge representative for a vessel frequently used by the offshore industry as a lay barge or crane vessel. The main particulars for the barge are listed in Table No. 1 below.

Length	(m)	150
Beam	(m)	50
Draft	(m^3)	10
Displaced volume	(m)	73750
C.G. above base	(m)	10
Transverse gyradius	(m)	20
Longitudinal gyradius	(m)	39
Vertical gyradius	(m)	39
Natural heave period	(sec)	10.4
Natural pitch period	(sec)	12.1
Natural roll period	(sec)	9.4

Table 1. Particulars of rectangular barge.

The discretization of the barge can be seen in Fig. 5.

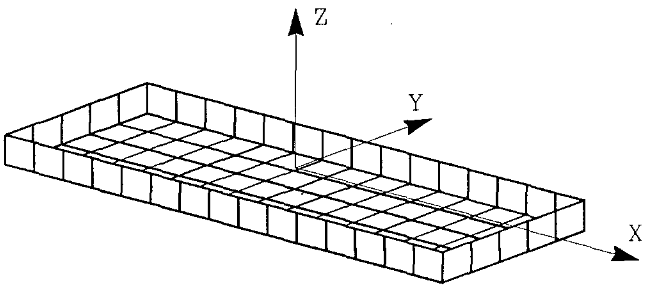

Figure 5. Sketch of wetted surface of the barge. xy-plane situated in SWL.

In the following calculations the barge is floating freely in all six degrees of freedom and it is exposed to regular, linear beam waves. The incident waves are generated within the calculation domain.

The sway, heave and roll motion transfer functions are plotted in Fig. 6-8, where they are compared to the experimental values obtained by Östergaard.

Legend:
△ Experiment
▲ Bemship

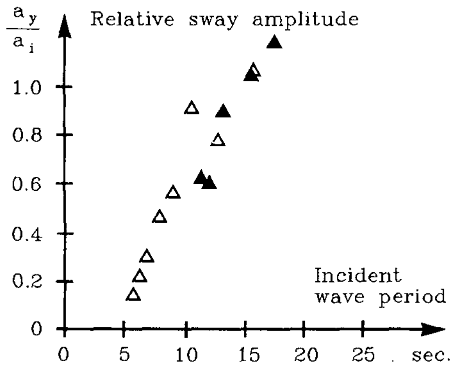

Figure 6. Comparison of calculated and experimental sway motions of the barge in beam waves. a_y and a_i are the amplitude of sway and the incident wave, respectively.

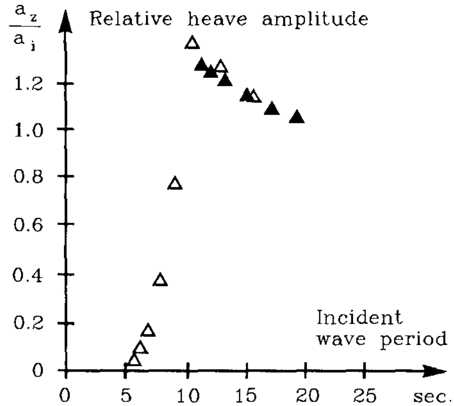

Figure 7. Comparison of calculated and experimental heave motions of the barge in beam waves. a_z and a_i are the amplitude of heave and the incident wave, respectively.

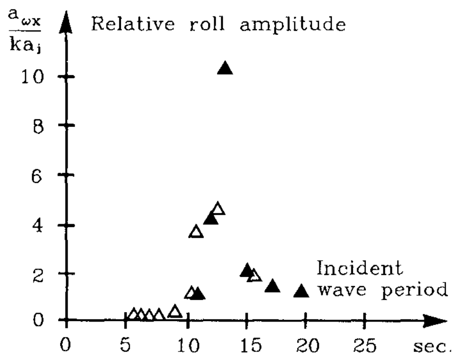

Figure 8. Comparison of calculations and experimental roll motions of the barge in beam waves. $a_{\omega x}$ and a_i are the amplitude of roll and the incident wave, respectively, k is the wave number $k = 2\pi/L$.

The barge is again floating freely, but is now exposed to regular, linear head waves.

The surge, heave and pitch motion transfer functions are plotted in Fig. 9-11, where they again are compared to the experimental values obtained by Östergaard.

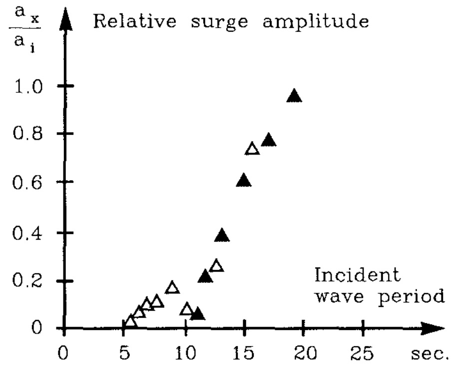

Legend:

△ Experiment
▲ Bemship

Figure 9. Comparison of calculated and experimental surge motions of the barge in head waves. a_x and a_i are the amplitude of surge and the incident wave, respectively.

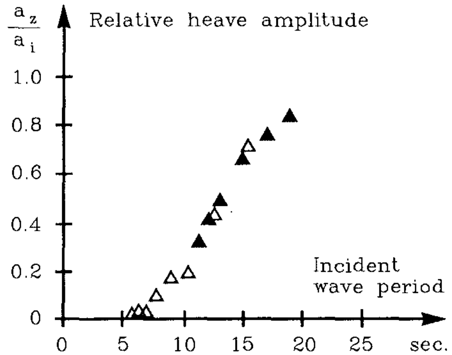

Figure 10. Comparison of calculated and experimental heave motions of the barge in head waves. a_z and a_i are the amplitude of heave and the incident wave, respectively.

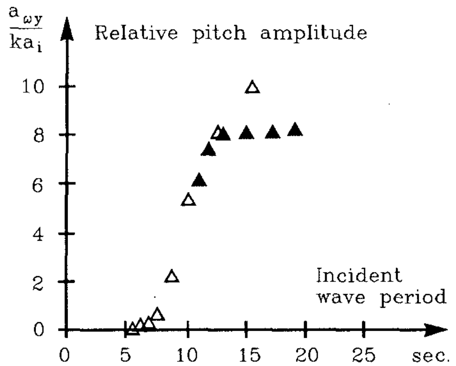

Figure 11. Comparison of calculated and experimental pitch motions of the barge in head waves. $a_{\omega y}$ and a_i are the amplitude of pitch and the incident wave, respectively, k is the wave number $k = 2\pi/L$.

When looking at the calculated and experimental measured barge motions in Figs. 6-11, a good agreement is found despite the rather low spatial resolution ($10 \cdot 10\ m^2$) of the body. Wave periods lower than 11 *sec.* are not used, as a spatial resolution of at least 16-18 elements per wave length is needed.

Conclusion

A new approach to the calculation of nonlinear drift forces on large bodies is reported. The numerical model is working in the time domain and the drift forces are calculated by filtering of long time series of the nonlinear lateral wave force acting on the body.

The nonlinear 2D version of the model is used to calculate steady drift forces as well as slowly varying drift forces.

Excellent agreement is found between the numerical results and the corresponding analytical solutions when the steady drift force (regular waves) and the mean drift force (beating waves) are considered.

In case of beating waves the preliminary results indicates that the amplitude of the slowly varying drift force may be somewhat underestimated by Newman's approximation.

An improved modelling of the absorption of the wave energy at the open boundaries is, however, probably required if the forces corresponding to deep water, irregular waves are to be calculated satisfactorily.

The linear version of the 3D model BEMSHIP is shown to yield good estimates of the motions of a freely floating barge exposed to head or beam waves.

References

Brorsen, M., 1989. *Numerical Model of the Nonlinear Interaction of Waves and Fixed Bodies.* Proceedings, IAHR XXIII Congress, Ottawa, Canada.

Brorsen, M.and Larsen, J., 1987. *Source Generation of Nonlinear Gravity Waves with the Boundary Integral Equation Method.* Coastal Eng. 11 : 93-113.

Faltinsen, O. M. and Løken, A. E., 1979. *Slow drift oscillations of a ship in irregular waves.* Applied Ocean Research, Vol. 1, No. 1 : 3-13.

Isaacson, M. de St. Q., 1982. *Nonlinear Wave Effects on Fixed and Floating Bodies.* J. Fluid Mech. 120 : 267-281.

Longuet-Higgins, M.S., 1977. *The mean forces exerted by waves on floating or submerged bodies with the applications to sand bars and wave power machines.* Proc. R. Soc. Lond. A : 463-480.

Standing, R.G., Dacunha, N.M.C and Matten, R.B., 1981. *Slowly-Varying Second-Order Wave Forces: Theory and Experiment.* NMI report R138, National Maritime Institute, UK.

Östergaard, C. and Schellin, T. E., 1987. *Comparison of Experimental and Theoretical Wave Motions on Floating and Compliant Structures.* Applied Ocean Research, Vol. 9, No. 4 : 192-213.